

D. Heeschen

PROGRESS REPORT
ON
WATER VAPOR EMISSION STUDIES

B. A. MANCHESTER

Two 23 GHz switched receivers, mounted on telescopes one and two of the interferometer, monitor emission from atmospheric water vapor in line-of-sight of the telescopes. Fluctuations in atmospheric water vapor are known to produce phase variations in a signal, a change of 1 mm in precipitable water vapor inducing a 20° phase change, and it is hoped that corrections for these variations can be made.

Each radiometer is switched between local oscillator frequencies of 20.8 GHz and 23.0 GHz at a switch rate of 10 Hz. Prior to January 27, 1970, the frequencies used were 20.3 GHz and 23.3 GHz. The receivers utilize a crystal mixer with no image rejection and I.F. passbands of 30 MHz to 280 MHz. A three-foot parabolic reflector is used with each receiver. The receiver double-sideband noise temperature is 1500°K , the output time constant is 10 seconds, and the theoretical RMS temperature uncertainty is $.04^\circ\text{K}$. [1]

The output from each receiver is sampled once a minute by the computer, and noise-tube calibration signals of $60 \pm 2^\circ\text{K}$ are fired by the operator approximately every three hours. The calibration signals are used to convert each receiver output from counts to $^\circ\text{K}$ antenna temperature. Then for each minute of data, output from telescope 1 is subtracted from that from telescope 2 to give net water vapor in line-of-sight of telescope 2. This quantity is cross correlated with the phase for telescopes 1 and 2, for each calibrator source scan. Excess water vapor observed by telescope 2 should increase the path length of the signal from source to telescope, thus producing a positive phase change; excess water vapor observed by telescope 1, giving a negative phase change. High positive correlation coefficients therefore indicate a close relationship between phase and water vapor fluctuations. Examples of data selected for high correlation are shown in figures 1 - 3. Parameters for these scans will be found in rows 3, 4 and 5 of Tables 1 and 2.

Data have been analyzed for the period of operation of the receivers, mid-October to the present time. For the period mid-October to the end of November both the phase and net water vapor showed large fluctuations, but the winter months' data are much less variable. Quite a number of scans with high correlation coefficients have been examined. Preliminary calibration of the telescope 1 receiver with an infra-red hygrometer indicates that a change of 1°K antenna temperature in water vapor is equivalent to a change of 0.8 mm of water vapor, and should induce a 16° phase change. The theory [2] predicts a change in brightness temperature of approximately 4°K for an increase of 1 mm in precipitable water vapor, so that it appears that further calibration of the receivers is necessary.

One would expect that a constant scale factor K, possibly close to 5, would give the best correction to phase, where corrected phase at time i, ϕ_i , is given by

$$\phi_i = \phi_i - KW_i = \phi_i - K(W2_i - W1_i),$$

where ϕ_i is observed phase,

W_i is net water vapor.

In examining scans with high positive cross correlation coefficients, it is found that the RMS phase can be reduced by significant amounts, but the scale factor giving the best results varies over a wide range from scan to scan. In Table 1 parameters for all calibrator source scans in the scan range 5500 - 5590, made over a period of 65 hrs. in November, are listed. This scan range includes some of the best correlated scans obtained. The reason for the large variation in scale factors is not clear, and it precludes the possibility of making on-line corrections to the phase.

Unfortunately, calibrator source scans usually yield only 16-20 data points, so that the significance of the calculated value of the correlation coefficient, r, should be examined. Using the t-distribution, one can test r to see if it is significantly different from zero. With the .02 level of significance for a sample size of 18, $r \geq .54$ implies that the value of r is significant. It is also possible to calculate the 95% confidence intervals for the population, or true, correlation coefficient ρ , given the sample correlation coefficient r and the sample size. For a sample size of 18, the ranges of ρ for given values of r are

$$\begin{array}{ll}
 r = 1.0 & , \quad \rho = 1 \\
 0.8 & , \quad 0.5 < \rho < 0.9 \\
 0.6 & , \quad 0.2 < \rho < 0.8 \\
 0.5 & , \quad 0.0 < \rho < 0.8.
 \end{array}$$

It is also possible to increase the cross-correlation coefficient, and hence further decrease the RMS phase, of scans by varying the weight attached to the output of the receivers. This could be interpreted as adjusting the gain of the receiver which should be correct to 6% as calibration marks are always used to scale the data. However, the scatter in gain factors is much greater than this. To obtain the data given in Table 2, for the same scan range as in Table 1, the phase was cross-correlated with the expressions

$$\begin{array}{l}
 (GF2) W2 - W1 \\
 \text{and} \quad W2 - (GF1) W1,
 \end{array}$$

where $W1$ is the output of receiver 1 in $^{\circ}K$,

$W2$ is the output of receiver 2 in $^{\circ}K$,

and $GF1$, $GF2$ were in turn allowed to vary between 0.0 and 1.0. As can be seen, significant improvements were made in cross-correlation coefficients for some scans, particularly those for which one of the gain factors was close to zero. This indicates that, at times, phase was much better correlated with output from one of the receivers than with the net output.

This phase was again corrected using the new formula

$$\phi_i = \phi_i - K (GF2W2_i - GF1W1_i),$$

for the values of $GF1$, $GF2$ given in Table 2, and the results are given in columns 5,6, and 7.

Scans made from zenith to horizon at H.A. zero on January 15th, with telescope separation of 2700 m, gave the following expressions for variation of water vapor with zenith angle

$$W1 = 6.36 \sec Z - 9.09$$

$$W2 = 3.16 \sec Z - 0.02$$

The receivers obey a linear sec Z relationship, and the slope of the line indicates the amount of water vapor present. Assuming that each receiver "saw" the same amount of water vapor (the sky was clear, and difference in elevation of the two telescopes produces a negligible effect) these relationships indicate that the efficiency of receiver 1 is approximately twice that of receiver 2. For other days with not such good data, the ratio of efficiencies (1:2) is found to be

22nd October 1:0.9

16th November 1:1.1

It seems therefore that receiver characteristics may be changing and this may explain the scatter in gain factors.

In a number of cases, the relationship between phase and water vapor variations is practically absent. Scans with high RMS water vapor and high RMS phase but low correlation, with high RMS phase but low RMS water vapor, and with low RMS phase but high RMS water vapor, are found. Two examples of each of these situations are shown in figures 4 to 9 inclusive, the parameters for the scans being given in Table 3. The three well-correlated scans in figures 1 to 3 make an interesting comparison. Explanations for these unpromising scans possibly lie in better understanding of receiver instabilities.

From the partial success of this project, it appears that the correction on-line of phase instabilities due to water vapor fluctuations is feasible, but not possible at present. Further calibration of both receivers with infra-red hygrometers, together with more data on receiver stability with time seem to be the main needs at present. The receivers and reflectors have now been taken down from the telescopes and will be installed side by side, enabling a comparison of their responses to fluctuations to be made.

Acknowledgments

I would like to thank Dr. D. Hogg and Dr. S. Weinreb for their assistance in preparing this report.

References

- [1] Dolan, J.L., General Description and Operating Instructions for the Water Vapor Receiver, N.R.A.O. Electronics Division Internal Report No. 89, January 1970.

- [2] Waters, J.W., Atmospheric Effects on Radio Wave Phase and the Correction of Vapor-Caused Phase Fluctuations by Radiometric Measurements of Water Vapor Emission, N.R.A.O. V.L.A. Scientific Memorandum No. 8, September 1967.

TABLE 1

Scan No.	Cross Correlation Coefficient	Scale Factor K	RMS Phase	Corrected RMS Phase	Reduction in RMS Phase	% Reduction in RMS Phase
5500	.533	4	11.22	9.49	1.73	15.4
5502	-.294	-4	12.69	12.12	.57	4.5
5504	.800	42	33.77	20.28	13.49	40.0
5506	.898	12	16.89	7.43	9.46	56.0
5509	.719	5	9.54	6.63	2.91	30.5
5512	.599	5	5.89	4.72	1.17	19.9
5514	.516	8	6.22	5.32	.90	14.5
5521	.239	3	5.67	5.50	.17	3.0
5526	.153	1	3.74	3.69	.05	1.3
5530	.247	3	3.19	3.09	.10	3.1
5531	.190	2	4.63	4.55	.08	1.7
5533	.242	2	3.60	3.49	.11	3.2
5534	.470	1	4.36	3.90	.46	10.6
5535	.209	2	4.00	3.91	.09	2.3
5536	.557	10	5.23	4.34	.89	17.0
5537	.143	1	3.02	2.98	.04	1.3
5539	-.125	0	2.93	2.93	0	0.0
5541	-.322	-3	4.37	4.14	.23	5.3
5543	.549	3	2.74	2.29	.45	16.4
5545	.069	1	2.69	2.69	0	0.0
5547	.278	1	2.28	2.19	.09	3.9
5549	-.203	-1	2.65	2.65	0	0.0
5551	.088	0	2.30	2.30	0	0.0
5553	.374	3	3.75	3.48	.27	7.2
5555	.194	0	3.60	3.60	0	0.0
5557	-.167	-1	3.13	3.09	.04	1.3
5559	.529	2	7.23	6.14	1.09	15.1
5560	.235	1	4.58	4.52	.06	1.3
5561	.390	1	2.72	2.53	.19	7.0
5562	.073	0	5.24	5.24	0	0.0
5563	.607	2	3.54	2.88	.66	18.7
5564	-.211	0	2.55	2.55	0	0.0
5565	.436	1	5.88	5.29	.59	10.0
5566	.394	1	7.47	6.95	.52	14.0
5567	.592	2	14.96	12.05	2.91	19.5
5569	-.273	-2.5	5.46	5.26	.20	3.7
5571	.565	4	4.82	3.99	.83	17.2
5573(a)	.248	3	3.65	3.53	.12	3.3
5573(b)	.868	10	5.18	2.58	2.60	50.2
5575	.579	6	5.70	4.64	1.06	18.6
5577	-.878	-10	3.33	1.60	1.73	52.0
5579	.087	1	4.67	4.65	.02	0.4
5580	.075	1	4.41	4.40	.01	0.2
5583	.691	4	3.12	2.26	.86	27.6
5585	.408	6	8.94	8.17	.77	8.6
5587	-.105	-1	4.93	4.90	.03	0.6
5588	.288	2	5.45	5.22	.23	4.2
5589	.713	10	9.24	6.48	2.76	29.9

TABLE 2

Scan No.	Gain Factor for 85-1 GF1	Gain Factor for 85-2 GF2	Improved Cross Correlation Coefficient	New Scale Factor	Corrected RMS Phase	% Reduction in RMS Phase	Improvement in Cross Correlation Coefficient
5500	1.0	1.0	.533	4	9.49	15.4	0
5502	0.0	1.0	.142	3	12.56	1.0	.436
5504	0.6	1.0	.867	41	16.81	50.2	.067
5506	0.6	1.0	.919	17	6.65	60.6	.021
5509	0.6	1.0	.735	7	6.47	32.2	.016
5512	1.0	0.3	.657	6.5	4.44	24.6	.058
5514	1.0	0.7	.521	8	5.31	14.6	.005
5521	1.0	0.1	.390	17	5.26	7.2	.151
5526	1.0	0.0	.259	2	3.61	3.5	.106
5530	0.0	1.0	.421	4	2.90	9.1	.174
5531	1.0	0.0	.352	5	4.34	6.3	.162
5533	0.0	1.0	.363	3	3.36	6.7	.121
5534	1.0	0.5	.482	2	3.82	12.1	.012
5535	0.0	1.0	.379	4	3.70	7.5	.170
5536	1.0	0.2	.899	1	4.30	17.8	.342
5537	1.0	0.7	.146	1	2.98	1.3	.003
5539	1.0	0.0	.083	0	2.93	0.0	.208
5541	0.0	1.0	.248	3	4.23	3.2	.570
5543	0.7	1.0	.553	3	2.29	16.4	.004
5545	1.0	0.0	.663	5	2.02	24.9	.594
5547	1.0	0.45	.288	1	2.18	4.4	.010
5549	0.0	1.0	-.012	0	2.65	0.0	.191
5551	0.0	1.0	.252	1	2.23	3.0	.164
5553	0.4	1.0	.546	6	3.18	15.2	.172
5555	1.0	0.0	.265	1	3.48	3.3	.071
5557	1.0	0.0	.175	1	3.09	1.3	.342
5559	1.0	0.7	.535	3	6.14	15.1	.006
5560	0.5	1.0	.247	1	4.46	2.6	.012
5561	0.2	1.0	.562	2	2.27	16.5	.172
5562	0.6	1.0	.074	0	5.24	0.0	.001
5563	0.5	1.0	.639	2	2.77	21.8	.032
5564	1.0	0.0	-.038	0	2.55	0.0	.173
5565	0.9	1.0	.439	1	5.29	10.0	.003
5566	1.0	0.0	.536	1	6.35	15.0	.142
5567	0.7	1.0	.609	5	11.93	20.2	.017
5569	0.0	1.0	.403	1	5.29	10.0	.676
5571	1.0	0.8	.568	4	3.98	17.4	.003
5573(a)	0.4	1.0	.268	14.5	3.53	3.4	.020
5573(b)	1.0	0.8	.877	10	2.50	51.7	.009
5575	0.1	1.0	.766	10	3.68	35.4	.187
5577	1.0	0.0	.215	4.5	3.25	2.4	1.093
5579	0.0	1.0	.195	2	4.58	1.9	.108
5580	1.0	0.0	.499	10.5	3.82	13.4	.424
5583	0.7	1.0	.699	5	2.24	39.3	.008
5585	0.2	1.0	.803	20	5.47	38.8	.395
5587	1.0	0.0	.113	1.5	4.90	0.6	.218
5588	0.3	1.0	.334	4	5.14	5.7	.046
5589	0.7	1.0	.722	13.5	6.42	30.6	.009

TABLE 3

Scan No.	RMS Water Vapor	RMS Phase	Cross Correlation Coefficient	Remarks
5215	6.88	17.24	0.13	Large RMS phase and water vapor, but low correlation
7108	3.98	13.54	-0.06	
4824	0.85	13.78	0.10	Large RMS phase, but small RMS water vapor
5619	0.41	10.27	0.12	
5555	2.50	3.60	0.19	Large RMS water vapor, but small RMS phase
5564	2.41	2.55	-0.21	

10 X 10 TO THE INCH 46 0780
7 X 10 INCHES
KEUFFEL & ESSER CO.
MADE IN U.S.A.

Phase (°)
270
180
90

Antenna Temp (°K)
0
-10

Antenna Temp (°K)
20
10
0

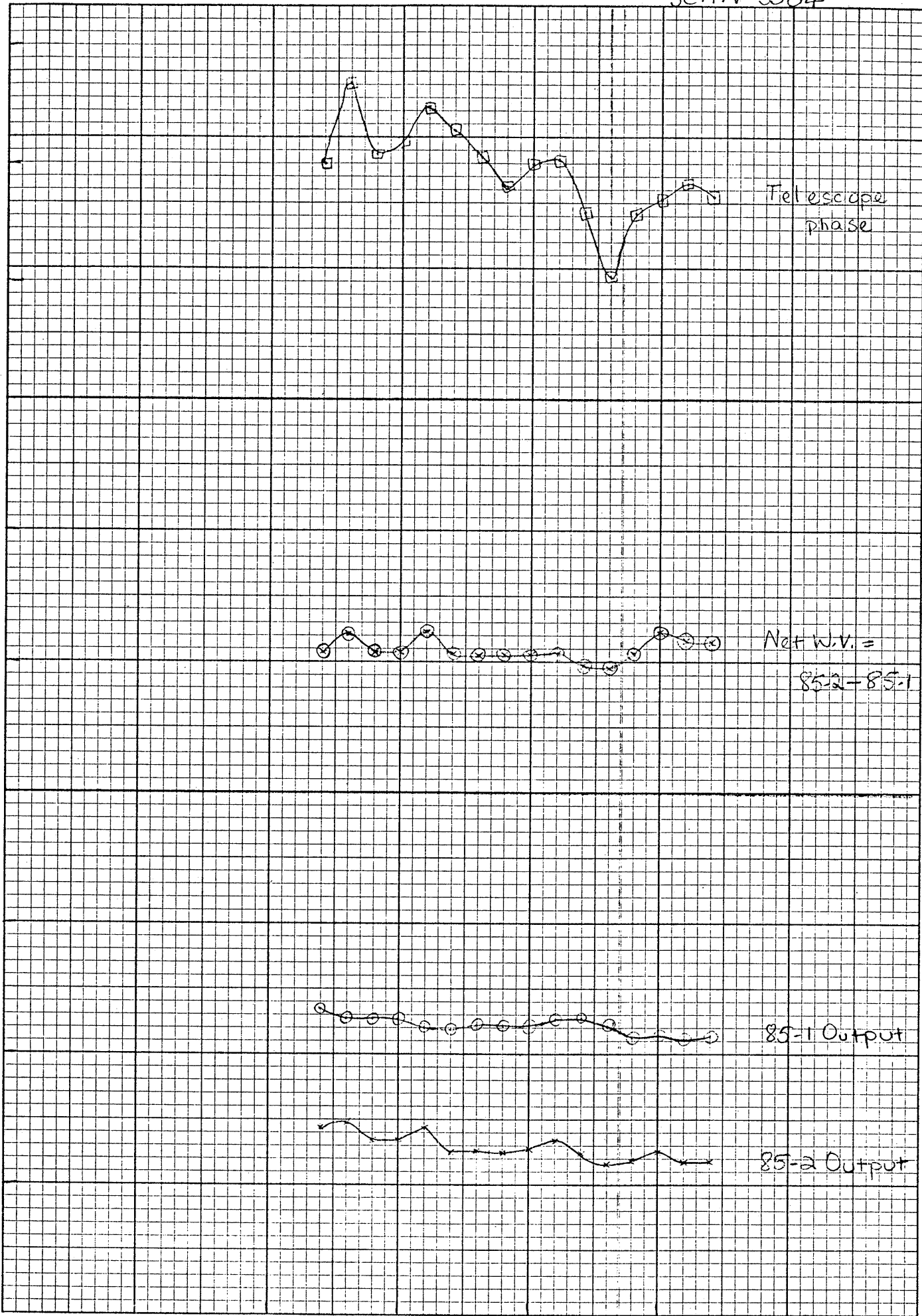


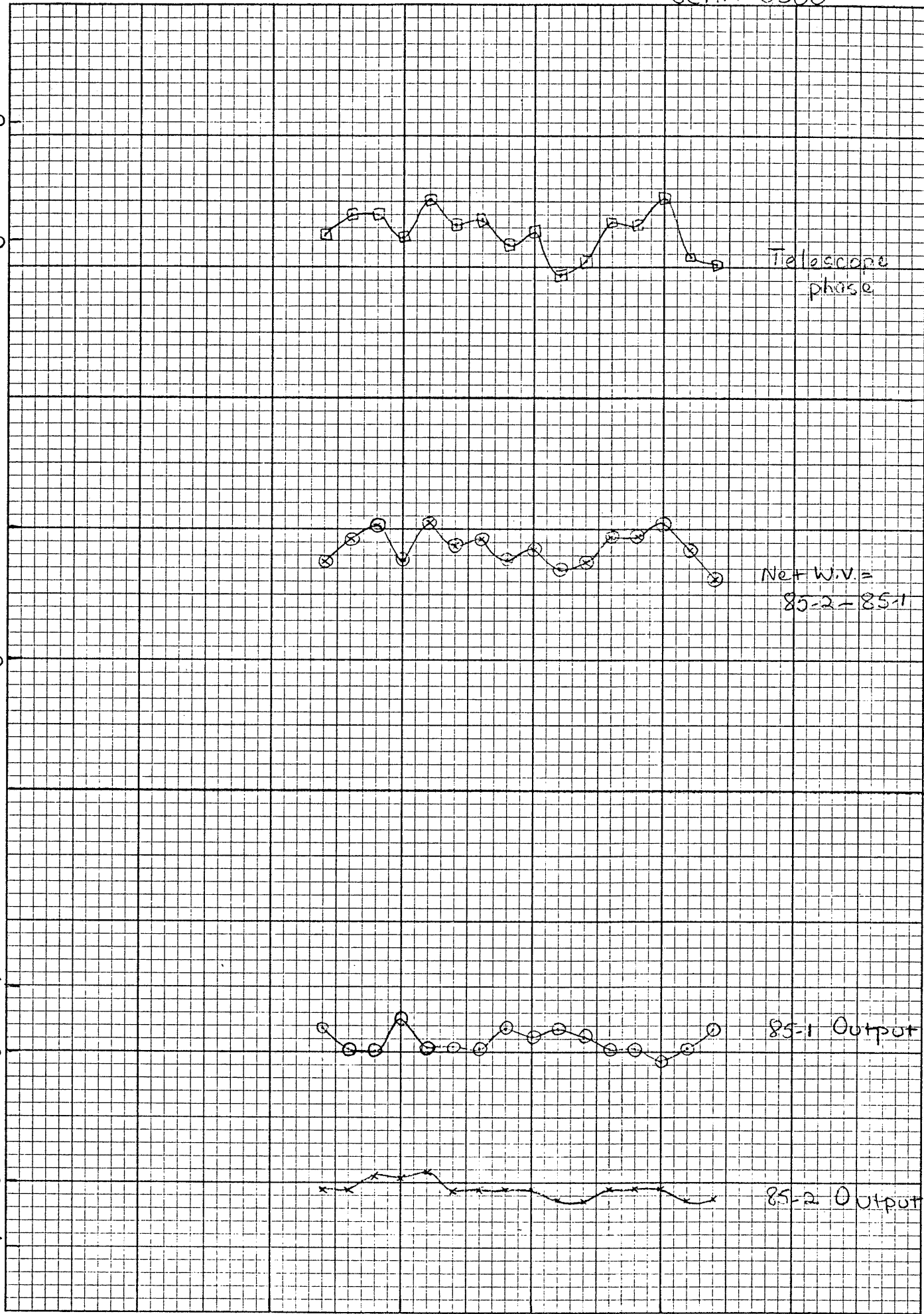
Fig 1.

KE 10 X 10 TO THE INCH 46 0780
7 X 10 INCHES MADE IN U.S.A.
KEUFFEL & ESSER CO.

Phase (°)

Antenna Temp (°K)

Antenna Temp (°K)



22h00m36s 05m 10m 15m

L.S.T.

Fig 2.

KE 10 X 10 TO THE INCH 46 0780
7 X 10 INCHES MADE IN U.S.A.
KEUFFEL & ESSER CO.

Phase (°)

Telescope
phase

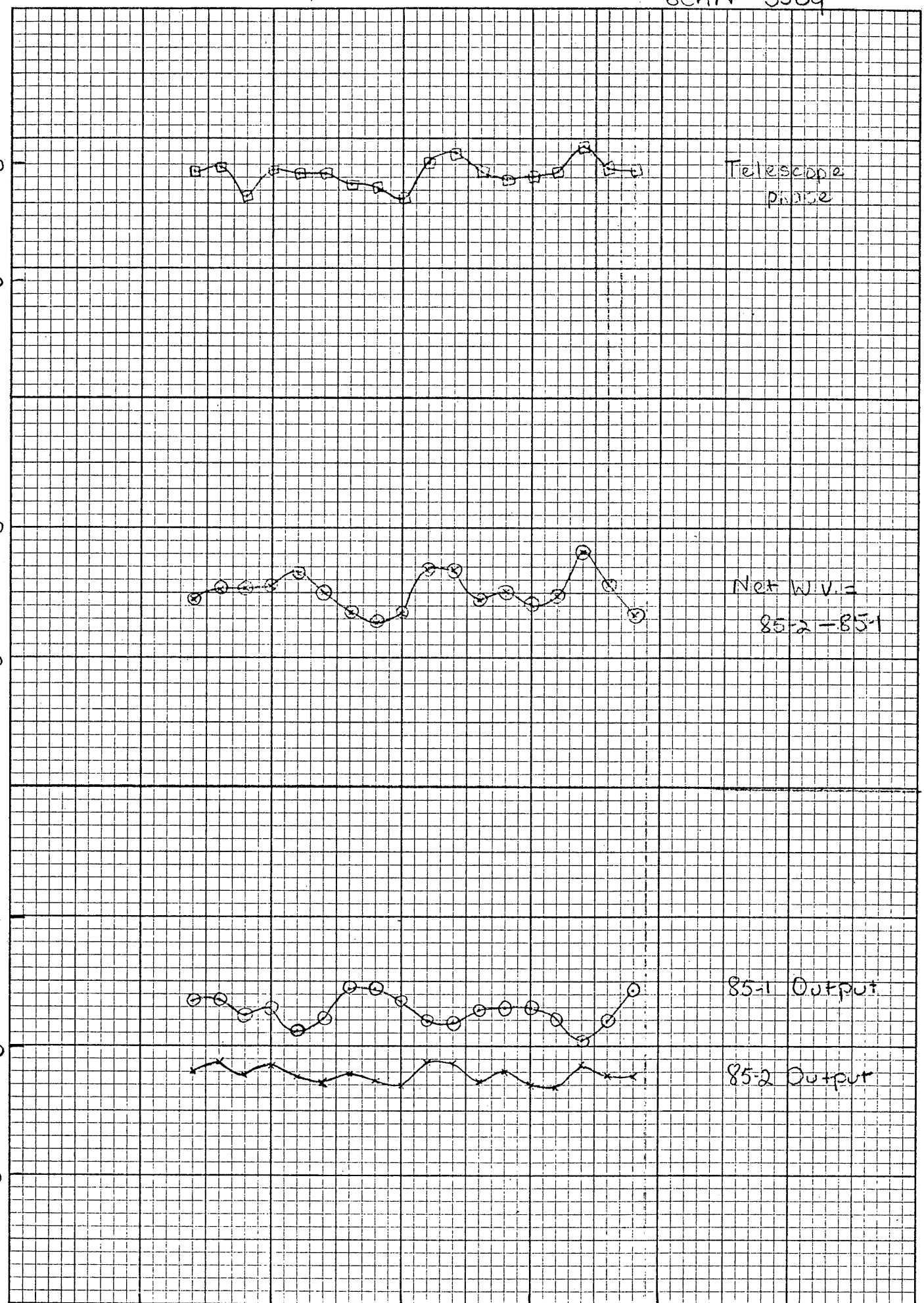
Antenna Temp (°K)

Net W.V. =
85-2 - 85-1

Antenna Temp (°K)

85-1 Output

85-2 Output



L.S.T.

Fig. 3.

KEE 10 X 10 TO THE INCH 46 0780
7 X 10 INCHES
KEUFFEL & ESSER CO.
MADE IN U.S.A.

Phase (°)

Antenna Temp (°K)

Telescope
phase

Net W.V. =
85-2 - 85-1

Antenna Temp. (°K)

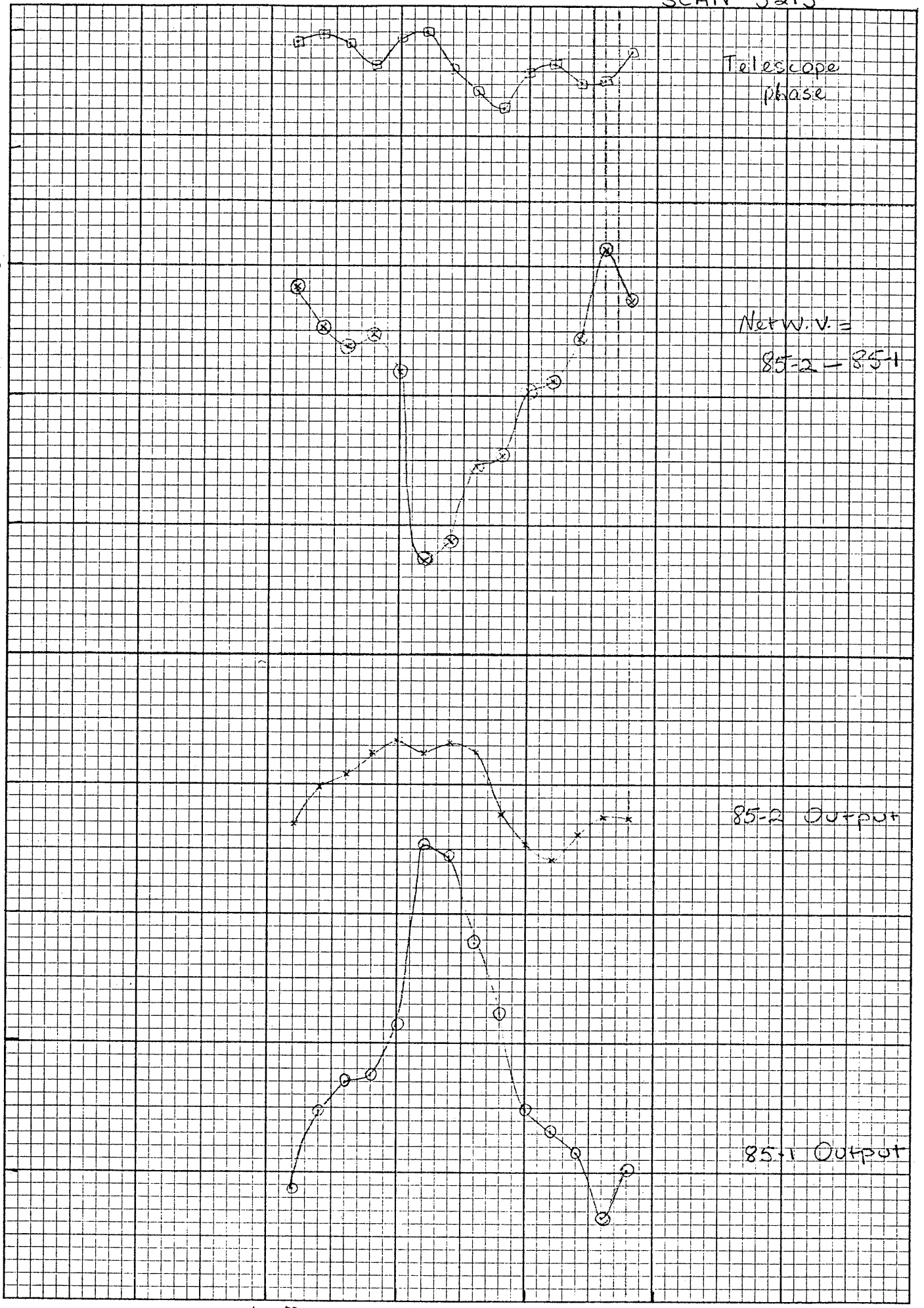
85-2 Output

85-1 Output

06^h00^m31^s 05^m 10^m 15^m

L. S. T.

Fig. 4.



KEE 10 X 10 TO THE INCH 46 0780
7 X 10 INCHES KEUFFEL & ESSER CO.
MADE IN U.S.A.

Phase (°)

Antenna Temp (°K)

Antenna Temp (°K)

Telescope phase

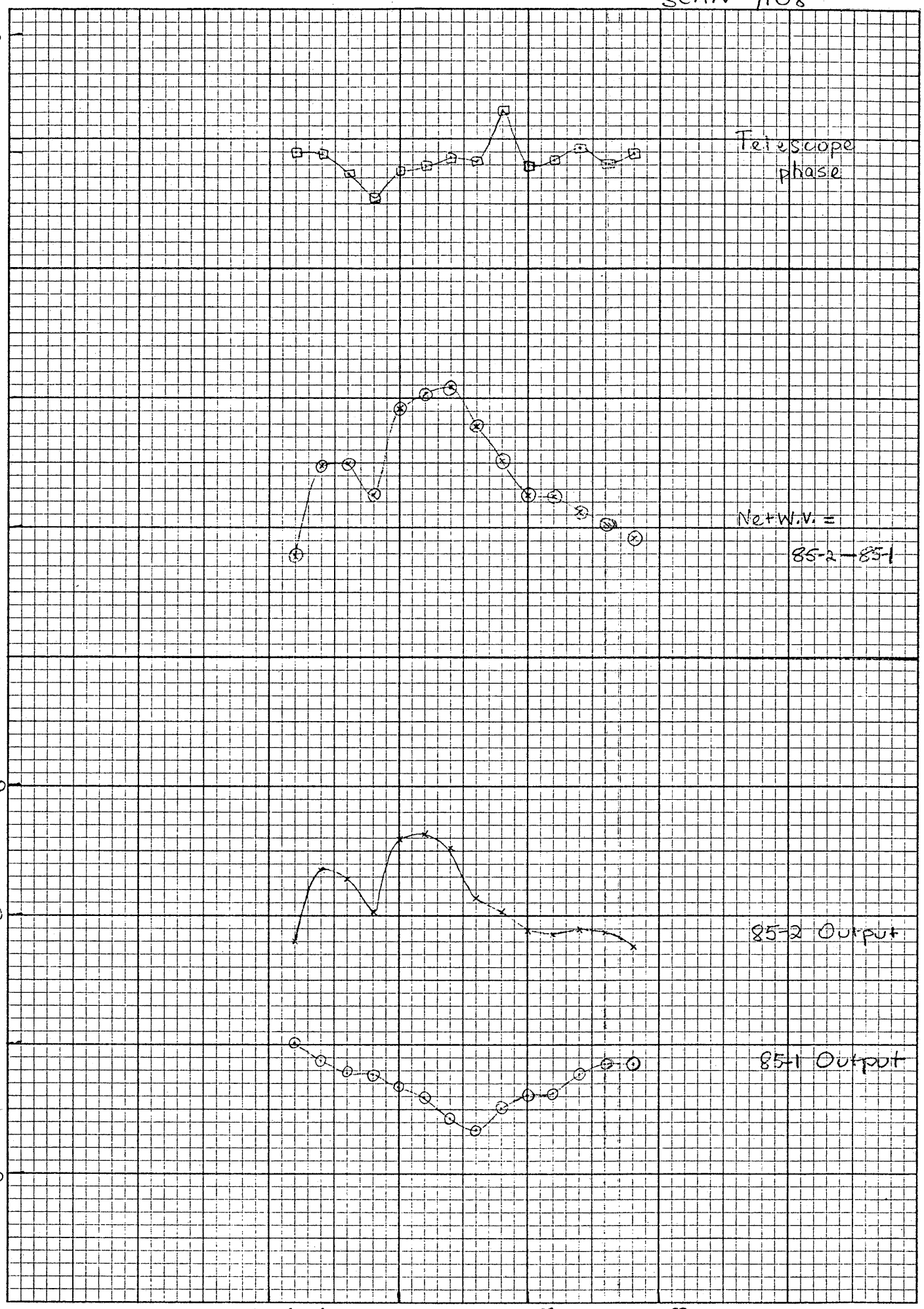
Net W.V. =
85-2-85-1

85-2 Output

85-1 Output

00^h 00^m 44^s 05^m L.S.T. 10^m 15^m

Fig. 5.



Phase (°)

Telescope
phase

Antenna Temp (°K)

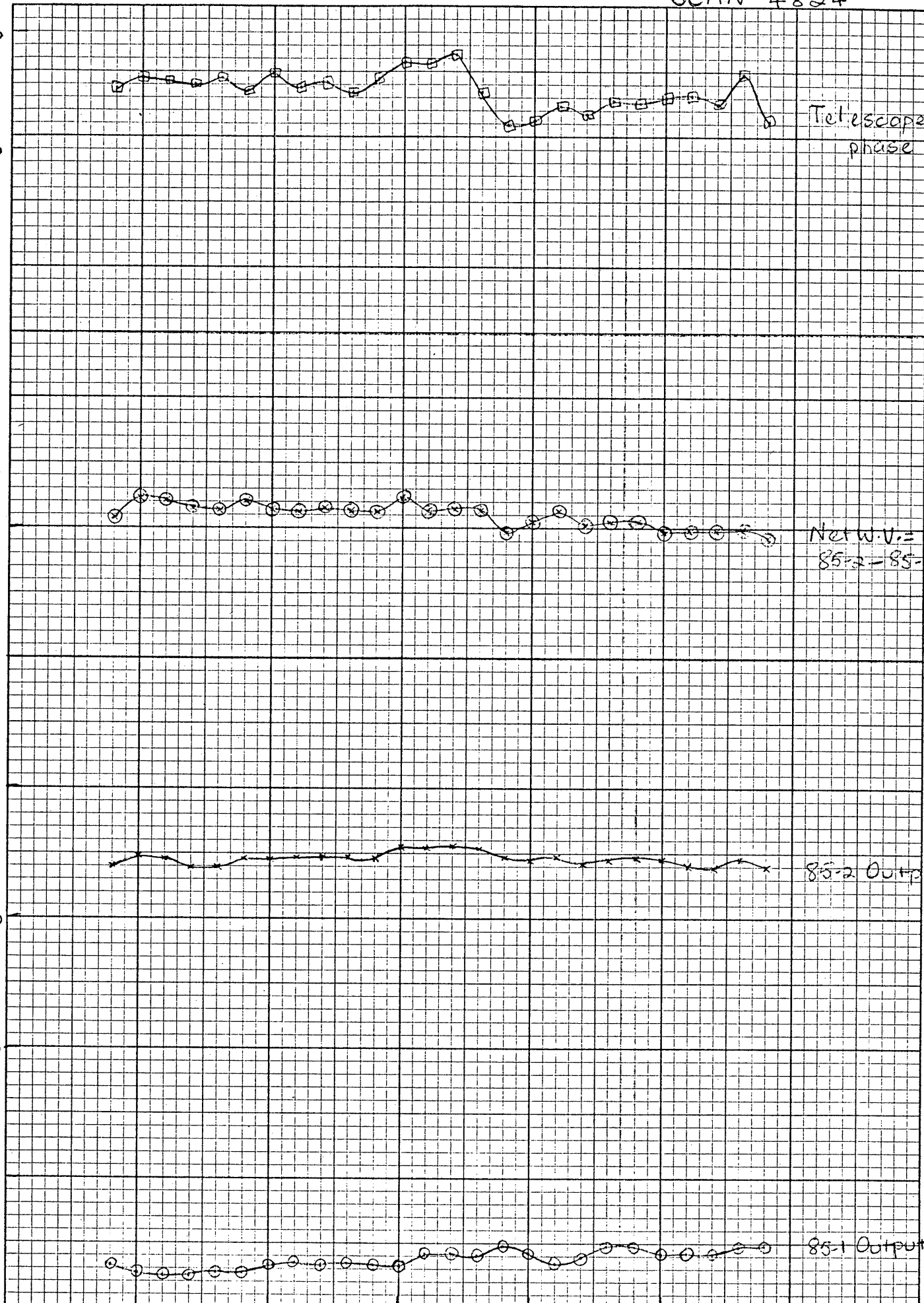
Net W.V. =
85-2-85-1

Antenna Temp (°K)

85-2 Output

85-1 Output

K&E 10 X 10 TO THE INCH 46 0780
7 X 10 INCHES
MADE IN U.S.A.
KEUFFEL & ESSER CO.



L.S.T. 17h 00m 11s Fig. 6.

KEUFEFFEL & ESSER CO.
MADE IN U.S.A.
46 0780
10 X 10 TO THE INCH
7 X 10 INCHES

Phase (°)

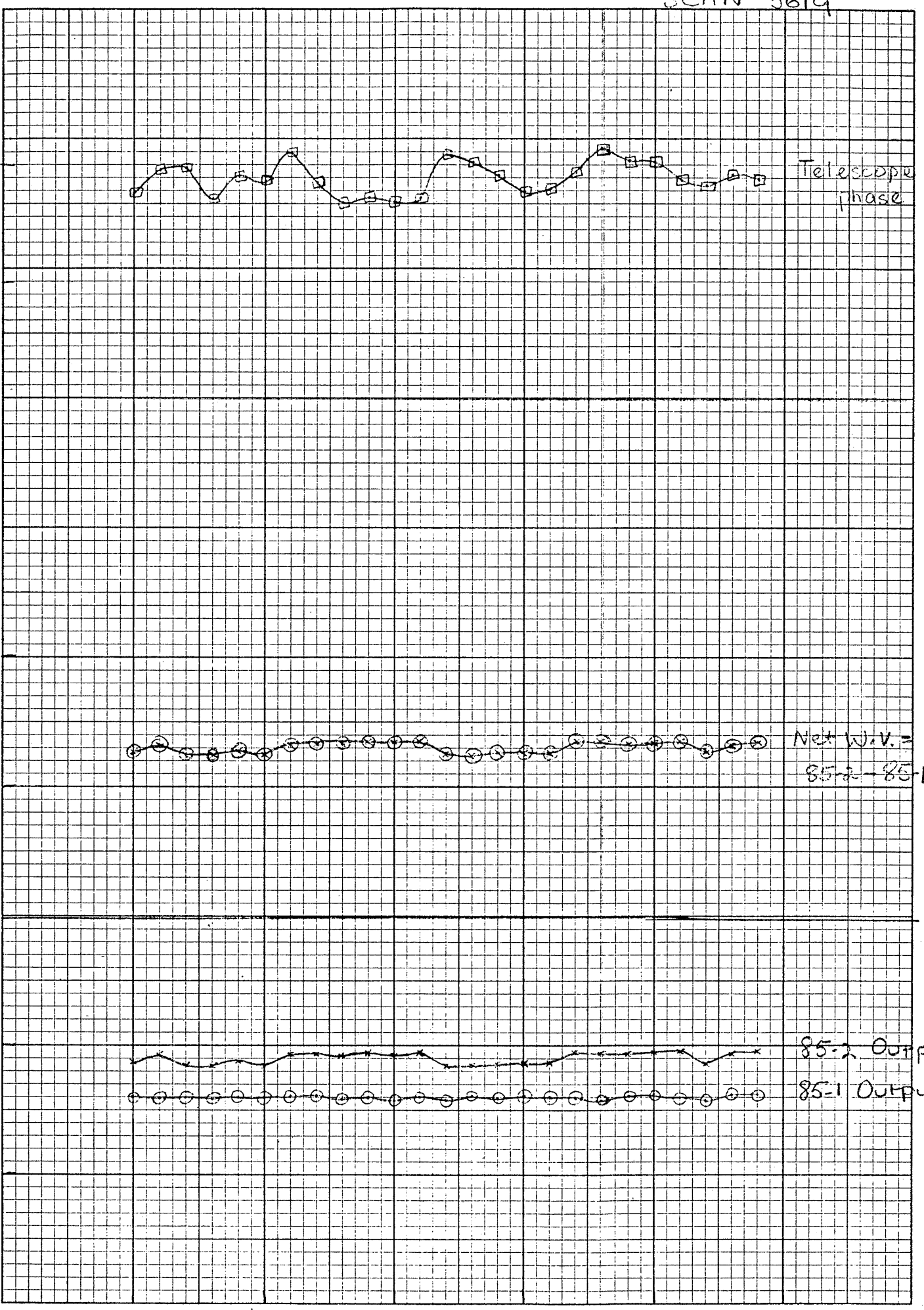
Antenna Temp (°K)

Antenna Temp (°K)

Telescope phase

Net W.V. = 85-2-85-1

85-2 Output
85-1 Output



55m 14^h00^m32^s 05m 10m 15m 20m L.S.T. Fig. 7.

10 X 10 TO THE INCH 46 0780
7 X 10 INCHES
KEUFFEL & ESSER CO.
MADE IN U.S.A.

Phase (°)
90
-180

Telescope
phase

Antenna
Temp (°K)
10
-20

Net W.M.
352-851

Antenna
Temp (°K)
30
20
10

85-1 Output

85-2 Output

07^h40^m38^s 45^m 50^m 55^m 08^h00^m38^s

L.S.T.

Fig. 8.



Phase (°)

Telescope
Phase

Antenna Temp (°K)

Net W.V. =
85-2-85-1

Antenna Temp (°K)

85-1 Output

85-2 Output

KE 10 X 10 TO THE INCH 46 0780
7 X 10 INCHES MADE IN U.S.A.
KEUFFEL & ESSER CO.

13^h15^m06^s 20^m 25^m 30^m 35^m 40^m 45^m
L.S.T.

Fig. 9.

